ISSN 1672-9145 **Acta Biochimica et Biophysica Sinica** 2007, **39**(11): 901–913 **CN** 31-1940/Q

EDTA-induced Membrane Fluidization and Destabilization: Biophysical Studies on Artificial Lipid Membranes

Virapong PRACHAYASITTIKUL[1]*, Chartchalerm ISARANKURA-NA-AYUDHYA[1], Tanawut TANTIMONGCOLWAT[1], Chanin NANTASENAMAT[1], and Hans-Joachim GALLA[2]

[1] *Department of Clinical Microbiology, Faculty of Medical Technology, Mahidol University, Bangkok 10700, Thailand;*
[2] *Institute of Biochemistry, Westfälische Wilhelms Universität, Muenster 48149, Germany*

Abstract The molecular mechanism of ethylenediaminetetraacetic acid (EDTA)-induced membrane destabilization has been studied using a combination of four biophysical techniques on artificial lipid membranes. Data from Langmuir film balance and epifluorescence microscopy revealed the fluidization and expansion effect of EDTA on phase behavior of monolayers of either 1,2-dipalmitoyl-*sn*-glycero-3-phosphocholine (DPPC) or mixtures of DPPC and metal-chelating lipids, such as N^{α},N^{α}-Bis[carboxymethyl]-N^{ε}-[(dioctadecylamino)succinyl]-*L*-lysine or 1,2-dioleoyl-*sn*-glycero-3-[*N*-(5-amino-1-carboxypentyl iminodiacetic acid) succinyl]. A plausible explanation could be drawn from the electrostatic interaction between negatively charged groups of EDTA and the positively charged choline head group of DPPC. Intercalation of EDTA into the lipid membrane induced membrane curvature as elucidated by atomic force microscopy. Growth in size and shape of the membrane protrusion was found to be time-dependent upon exposure to EDTA. Further loss of material from the lipid membrane surface was monitored in real time using a quartz crystal microbalance. This indicates membrane restabilization by exclusion of the protrusions from the surface. Loss of lipid components facilitates membrane instability, leading to membrane permeabilization and lysis.

Keywords ethylenediaminetetraacetic acid; film balance; atomic force microscopy; quartz crystal microbalance; membrane fluidization and destabilization

Ethylenediaminetetraacetic acid (EDTA) is a hexadentate chelator capable of binding stoichiometrically to metal ions through four carboxylate and two tertiary amine groups [1]. For the last five decades, EDTA has been widely used in many applications as a drug of choice for metal-overload, anti-oxidative stress, and anti-aging [2–4]. The disodium or calcium disodium salt forms have been approved by the US Food and Drug Administration as food additives [5]. EDTA prevents deteriorative effects in food and preserves color, odor, and flavor [6]. In cosmetics and pharmaceuticals, EDTA is primarily added as a stabilizer to prevent adverse effects in metals. The calcium sequestering effect of EDTA has long been used as an anticoagulant for blood sampling. Recent studies show high feasibility of using NaFeEDTA and Na_2EDTA as iron fortification compounds to increase iron absorption to treat iron deficiency anemia [7]. An acceptable daily intake of EDTA is 2.5 mg per kg of body weight as recommended by the Food and Agriculture Organization of the United Nations and the World Health Organization. The level of additive for food and cosmetics ranges from 25 to 500 ppm. Although current data suggest that EDTA is safe to be used in foods and other consumer products, adverse effects of EDTA remain unclear. Induction of oxidative stress and cell apoptosis by EDTA has been reported [8, 9]. Long-term exposure to EDTA leads to interstitial

Received: March 22, 2007 Accepted: May 22, 2007

This work was supported by the grants from the Deutsche Forschungsgemeinschaft and the Bundesministerium für Wirtschaftliche Zusammenarbeit und Entwicklung (Federal Ministry for Economic Co-operation and Development) (No. GA233/19-1,2), also from the Thailand Toray Science Foundation and the Thailand Governmental Budget of Mahidol University (No. 02012053-0003)

*Corresponding author: Tel, 662-849-6318; Fax, 662-849-6330; E-mail, mtvpr@mahidol.ac.th

DOI: 10.1111/j.1745-7270.2007.00350.x

hemorrhage, tissue injury and renal necrosis [10–12]. A study on an animal model reveals that EDTA disrupts tight junction and membrane integrity of rabbit cellular membranes [13].

In Gram-negative bacteria, EDTA and other metal chelators [*e.g.*, IDA, nitrilotriacetic acid (NTA), CDTA, and HDTA] induce outer membrane permeabilization and cell lysis. Synergistic activity of EDTA with antimicrobials has been shown in several genuses of bacteria. It is believed that the metal chelator sets apart metal ions from the outer membrane, resulting in lipopolysaccharide and protein dissociation to lead to cell lysis [14–17]. However, detailed investigation of the molecular mechanism has not yet been revealed.

Herein, we apply four biophysical techniques, film balance, epifluorescence, atomic force microscopy (AFM), and quartz crystal microbalance (QCM), to elucidate the effect of EDTA on artificial lipid membranes. The film balance is effective for studying the interaction of phospholipids and surface-active materials by monitoring the isothermal behavior [18–20]. Nanoscale topographical changes of lipid membrane upon interaction with EDTA were visualized under AFM [21]. Kinetic interaction between EDTA and solid-supported artificial membranes can readily be monitored in real time using QCM [22]. These techniques provide a plausible mechanism of membrane destabilization by EDTA.

Materials and Methods

Lipids, proteins and chemicals

1,2-Dipalmitoyl-*sn*-glycero-3-phosphocholine (DPPC) and 1,2-dioleoyl-*sn*-glycero-3-[*N*-(5-amino-1-carboxypentyl iminodiacetic acid) succinyl] (NTA-DOGS) were purchased from Avanti Polar Lipids (Alabaster, USA) and used without further purification. N^{α},N^{α}-Bis [carboxymethyl]-N^{ε}-[(dioctadecylamino)succinyl]-*L*-lysine (NTA-DODA) [23–25] was a generous gift from Prof. Robert TEMPE (Max-Planck-Institut für Biochemie and Technische Universität, Berlin, Germany). Octanethiol was ordered from Fluka (Neu Ulm, Germany). Milli-Q water (18.2 MΩ/cm) was produced by passing normal water through a series of water purification systems consisting of a Milli-RO 10 Plus and a Milli-Q Plus 185 (Millipore, Eschborn, Germany). For the film balance and epifluorescence measurement, HEPES buffer (10 mM HEPES and 150 mM NaCl, pH 7.5) with and without 50 and 100 mM EDTA was used. Phosphate-buffered saline (PBS; 50 mM Na_2HPO_4 and 0.3 M NaCl, pH 7.4) was used in all AFM and QCM experiments. Lipid stock solutions were prepared by dissolving powdered lipid in chloroform as indicated elsewhere [20]. For AFM experiments, the mixture of DPPC with NTA-DOGS (DPPC:NTA-DOGS) at a ratio of 4:1 was preloaded with zinc ions by adding an equimolar amount of $ZnCl_2{\cdot}2H_2O$ dissolved in methanol. For ease of representation, the colon (:) denotes lipid layer mixtures, and the forward slash (/) denotes lipid bilayers. For example, the mixture of DPPC with NTA-DOGS will be represented as DPPC:NTA-DOGS, and the lipid bilayer of DPPC and DPPC:NTA-DOGS will be represented as DPPC/DPPC:NTA-DOGS. This convention will be used throughout the article.

Chimeric green fluorescent protein carrying hexapolyhistidine (H_6GFP) was expressed in *Escherichia coli* strain TG1 and further purified to homogeneity by immobilized metal affinity chromatography charged with zinc ions as previously described [26,27].

Film balance and epifluorescence measurements

Measurements were carried out on a computer-controlled Wilhelmy film balance (Riegler and Kirstein, Mainz, Germany) with an operational area of 144 cm^2 and a bulk volume of 74 ml subphase at a constant temperature of 20 ºC. Prior to each experiment, a Langmuir trough was cleaned as described elsewhere [20]. Chloroform solution containing Bodipy-PC-doped DPPC or a lipid mixture with metal-chelating lipids was spread on the air/liquid interface of the HEPES buffer subphase containing 0, 50, or 100 mM EDTA using a Hamilton microsyringe. The solvent was allowed to evaporate for at least 10 min. After evaporation, the lipid monolayer was compressed at a constant compression rate (2.8 cm^2/min), accompanied with monitoring of surface pressure versus area per molecule. Until the surface pressure reached 45 mN/m, the lipid monolayer was expanded with the same rate as compression, to omit the collapsing of the monolayer.

An epifluorescence micrograph of the lipid monolayer was taken during the second round of compression. Briefly, 0.2 mol% Bodipy-PC-doped lipid monolayer was excited by a high-pressure mercury lamp (50 W) at 505 nm wavelength and visualized using an Olympus STM5-MJS light microscope (Olympus, Hamburg, Germany) equipped with a CCD camera using a 513 nm emission filter. Compression of the lipid monolayer was stopped at the desired surface pressure for approximately 1–5 min to record the lateral domain structure of the lipid monolayer.

Preparation of Langmuir-Blodgett bilayer on mica and AFM measurement

A Langmuir-Blodgett film was prepared using a Wilhelmy balance equipped with a 25 ml Teflon trough (15.4 cm×2.5 cm) and a dipper device (Riegler and Kirstein). DPPC was spread on the PBS buffer subphase. After an equilibration time of 10 min, the film was compressed at a constant compression rate (1.8 cm^2/min) with a surface pressure of 45 mN/m at the subphase temperature of 20 ºC. The DPPC monolayer was transferred at a speed of 0.7 mm/min to an atomically flat surface of a freshly cleaved mica sheet. The monolayer film was allowed to dry at atmospheric conditions overnight. The second layer was formed by dipping the first hydrophobic DPPC monolayer into a 40 mN/m preformed layer composed of DPPC and Zn^{2+}-NTA-DOGS complex (DPPC:Zn^{2+}-NTA-DOGS) at a ratio of 4:1 to obtain DPPC/DPPC:Zn^{2+}-NTA-DOGS. The mica sheet was then transferred into an open fluid cell under buffer solution.

Surface images of solid-supported DPPC/DPPC:Zn^{2+}-NTA-DOGS were obtained in an open fluid cell using AFM (Nanoscope IIIa Bioscope; Digital Instruments, Santa Barbara, USA) operating in contact mode and equipped with a 100 μm ×100 μm G-scanner. For topographical images, a commercially available microfabricated silicon nitride cantilever (NP-S; Veeco Instruments, Santa Barbara, USA) with an approximate tip radius of 10 nm and a spring constant of 0.06 N/m, was used. Minimal load force (200±400 pN) was carried out during contact mode imaging, and the scan rate was fixed at 1 Hz. A stock solution of EDTA dissolved in PBS was then injected into the open fluid cell to yield the final concentration of 5 mM and the surface alteration was observed at various time intervals. Multiple cross-sections of membrane protrusion by AFM were carried out and the mean height of individual protrusions was analyzed by the WSxM software (Nanotec Electronica, Madrid, Spain).

Vesicle preparation

The DPPC:NTA-DOGS layer was deposited on a QCM surface using the vesicle fusion technique [22]. Briefly, the lipid mixture was prepared by mixing a chloroform solution containing DPPC with NTA-DOGS at a 4:1 molar ratio. Solvent was allowed to evaporate under a stream of nitrogen gas at 60 ºC for 15 min followed by 2 h incubation under vacuum at 50 ºC. The lipid film was stored at 4 ºC until used. Unilamellar vesicles of DPPC:NTA-DOGS were obtained by swelling the lipid film in PBS followed by pressing the dissolved solution through a polycarbonate membrane (100 nm pore diameter) through a miniextruder (LiposoFast; Avestin, Ottawa, Canada).

Preparation of lipid bilayer on QCM surface

An AT-cut quartz resonator with a 5 MHz fundamental resonance frequency (KVG, Neckarbischofsheim, Germany) was coated on both sides with a gold electrode, each with a surface area of 0.265 cm^2. Prior to use, they were cleaned with piranha solution (60 ml concentrated H_2SO_4 and 20 ml of 30% H_2O_2), subsequently exposed to high-energy argon plasma (plasma cleaner; Harrick, Ossining, USA) for 5–10 min then placed into a Teflon chamber. The hydrophobicity of the gold electrode for vesicle fusion was introduced by incubation with ethanolic solution containing 1 mM octanethiol for 30 min. Unbound octanethiol was removed by rinsing with ethanol followed by PBS, five times each. The complete surface coverage was examined by impedance analysis [22]. The second layer of lipid membrane was prepared by exposing the hydrophobized QCM surface with DPPC:NTA-DOGS vesicles for 1 h at 50 ºC followed by storing at ambient temperature overnight to induce complete fusion. Remaining vesicles were removed by rinsing the electrode surface several times with buffer solution. Impedance analysis was redone to ensure proper formation of insulating phospholipids.

QCM measurement

The QCM measurement system consisted of a quartz crystal and was equipped with a Teflon holder to allow aqueous solution to contact with the membrane-coated surface on the quartz crystal [22]. The inlet and outlet of the Teflon holder was connected to a peristaltic pump to allow continuous exposure of the QCM surface to a flow of buffer and sample. The whole system comprised a 2 ml volume aqueous circuit pumped at a flow rate of 1.36 ml/min through the quartz chamber. The system was kept in a water-jacketed Faraday cage to minimize external RF interference with the QCM, and was equipped with a temperature-controlled circulatory water bath for maintaining the temperature at 20 ºC. The oscillation of the quartz crystal was controlled by an SN74LS124N integrated circuit (Texas Instruments, Dallas, USA). The voltage-controlled oscillator required 5 V of supply voltage to facilitate oscillation of the quartz crystal, which was connected to the silicon chip. The output resonance frequency was monitored by a Hewlett Packard frequency counter (HP 53181A; Hewlett Packard, Palo Alto, USA) and recorded on a personal computer through a data acquisition board from National Instruments.

Molecular model of DPPC-EDTA complex

The calculations were carried out using the quantum chemical software Spartan'04. Molecular mechanics and semiempirical PM3 method were used to obtain the proposed structure of the DPPC-EDTA complex. The molecular structure of DPPC and EDTA were drawn with the molecule-building module of Spartan'04. Two molecules of DPPC were placed in an arbitrary position in which the polar head group of DPPC was oriented near the EDTA molecule [28]. Next, the initial geometry of the DPPC-EDTA complex was subjected to preoptimization using the Merck Molecular Force Field, followed by full geometry optimization with the semiempirical PM3 method. Plausible electrostatic interactions of EDTA and the polar head group of DPPC were deduced from the geometrically optimized structure.

Results

Fluidizing effect of EDTA on lipid monolayer

Accordingly, our findings indicated that EDTA exerted a strong fluidizing effect on the lipid membrane. The experiment was initiated by investigation of the EDTA effect on the pressure-area isotherm of pure DPPC or lipid mixtures with metal-chelating lipids through the Langmuir film balance technique. The isotherms of the lipid monolayer in the absence and the presence of 50 and 100 mM EDTA are shown in **Fig. 1**. Typical phase transition of DPPC from the liquid expanding (*le*) to the liquid condensing (*lc*) phase was observed at 5 mN/m after the spreading of 99.8 mol% DPPC and 0.2 mol% Bodipy-PC onto the HEPES buffer subphase [**Fig. 1(A)**]. EDTA exerted no effect on the *le-lc* phase transition of the DPPC monolayer, but there were evident shifts to a higher area per molecule. The potent effect of EDTA on fluidity and expansion of the lipid monolayer was clearly revealed in a concentration-dependent manner. Specific molecular areas determined at 20 mN/m (A_{20}) were shifted from 48 to 60 and 71 Å^2 in the presence of 50 and 100 mM EDTA, respectively. This expansion can be attributed to the insertion of EDTA into the lipid monolayer. Further compression of up to 45 mN/m promoted a tightly packed DPPC. This partially excluded the EDTA from the film as indicated by the presence of the second plateau region at 45 mN/m. However, it should be noted that the remaining intercalated EDTA molecule on the lipid film was independent of the subphase concentration because the isotherms at 50 and 100 mM became identical at high surface pressure. Moreover, expansion of the monolayer arises from the ionic interaction between monovalent salt ions and the lipid head group. The pressure-area isotherm of the pure DPPC monolayer was shifted to the right when the water subphase was replaced with PBS [**Fig. 1(B)**].

The effect of EDTA on the isotherm of lipid mixtures of DPPC with saturated (NTA-DODA) or unsaturated (NTA-DOGS) metal-chelating lipids was further explored. A lipid monolayer, formed by spreading a mixture of DPPC, 20 mol% NTA-DODA, and 0.2 mol% Bodipy-PC (DPPC: NTA-DODA) over an EDTA-free subphase, showed similar isothermal behavior to that of the DPPC lipid membrane [**Fig. 1(C)**]. The *le-lc* phase transition was revealed at 5 mN/m surface pressure with slightly higher compressibility than DPPC. This similar isothermal property indicated homogeneous distribution of NTA-DODA on the DPPC monolayer due to the presence of two saturated hydrocarbon chains (18:0). The bulky metal chelator NTA, at the polar head group, influenced the compressibility. NTA is a negatively-charged metal chelator that might repel each ligand during film compression, causing a slight shift to a larger molecular area (A_{20}=50 Å^2). The presence of 50 and 100 mM EDTA in the buffer subphase was responsible for the fluidization effect and expansion of the surface area from 50 to 56 and 78 Å^2, respectively. Furthermore, the exclusion of EDTA from the lipid monolayer was observed at high compression pressure [**Fig. 1(C)**].

The isotherm of unsaturated metal-chelating lipids (DPPC:NTA-DOGS) showed drastic fluidization with an A_{20} of 56 Å^2 [**Fig. 1(D)**]. Dissipation of the typical *le-lc* phase transition was revealed while establishing a small plateau region at 10 mN/m. The unsaturated hydrocarbon tails of NTA-DOGS changed the phase behavior of the lipid mixture to a more disordered state. Changes of such behavior are caused by the kinks of the unsaturated hydrocarbon, which occupy a large surface area. There is steric hindrance during film compression. In the presence of EDTA, the plateau regions shifted to lower surface pressure (8 and 6 mN/m) when the EDTA concentration was increased from 50 to 100 mM. Formation of the *lc* at low surface pressure approaching the *le-lc* phase transition of DPPC suggests that EDTA induces the phase separation phenomenon by interacting with the DPPC head group and further segregates the DPPC-rich domain from the lipid mixture. Furthermore, the difference in isothermal behavior of DPPC and the unsaturated hydrocarbon chain of NTA-DOGS might also be taken into account. The fluidization and expansion of the surface area from 56 to

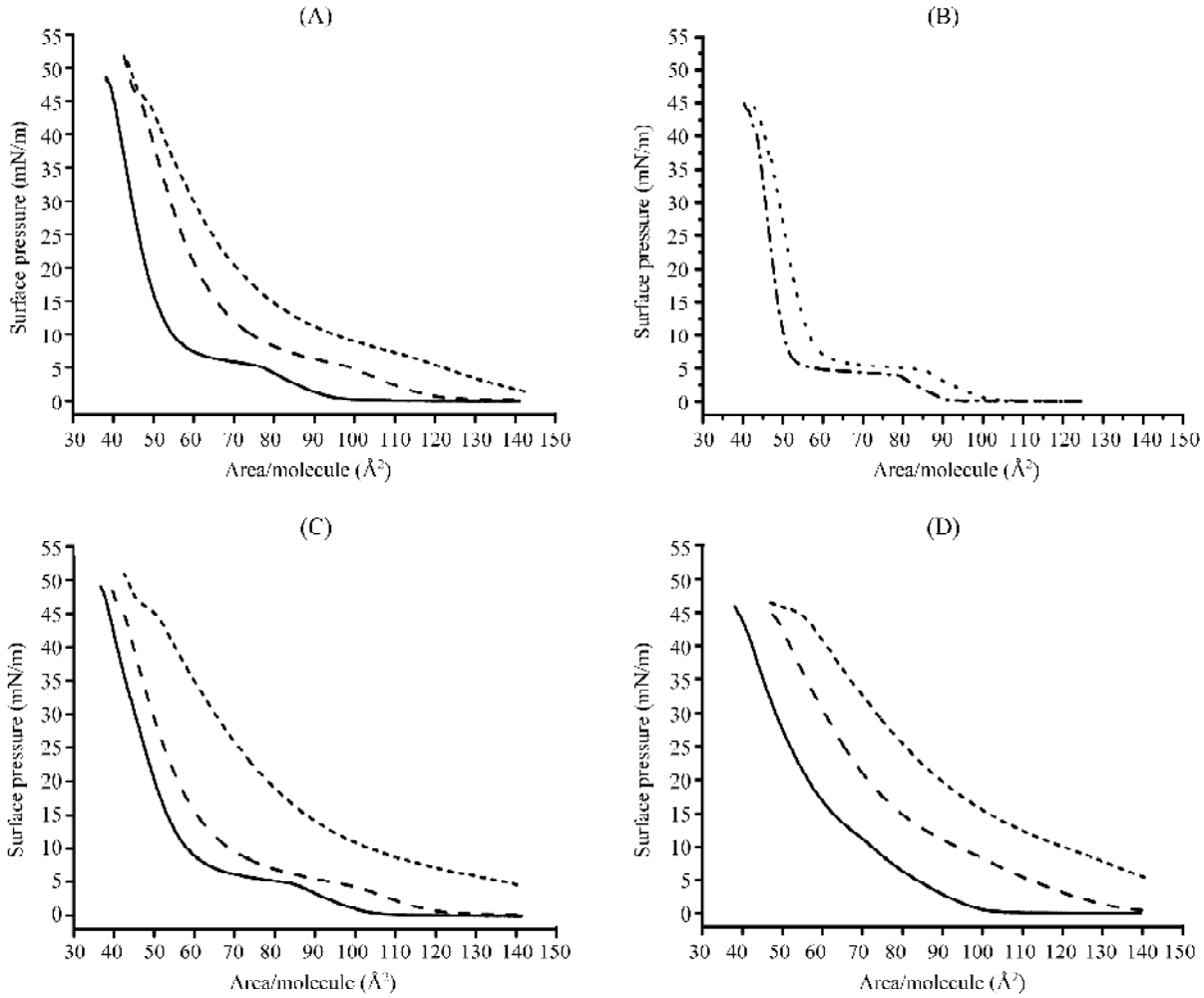

Fig. 1 EDTA effect on the pressure-area isotherm of pure 1,2-dipalmitoyl-*sn*-glycero-3-phosphocholine (DPPC) or lipid mixtures with metal-chelating lipids

Pressure-area isotherms of DPPC (A), DPPC:N^{α},N^{α}-Bis[carboxymethyl]-N^{ε}-[(dioctadecylamino)succinyl]-*L*-lysine (NTA-DODA) (C), and DPPC : 1,2-dioleoyl-*sn*-glycero-3-[*N*-(5-amino-1-carboxypentyl iminodiacetic acid) succinyl] (NTA-DOGS) (D) over the HEPES buffer subphase containing 0 mM (solid line), 50 mM (dashed line) and 100 mM (short dashed line) of EDTA. The pressure-area isotherm of DPPC spread on Milli-Q water (dash-dot line) and phosphate-buffered saline (dotted line) is shown in (B). HEPES buffer containing 50 or 100 mM EDTA was prepared by dissolving solid Na-EDTA, NaCl, and HEPES powder in deionized water and the pH was adjusted to 7.5 prior to use.

71 and 90 Å^2 was also observed in the presence of 50 and 100 mM EDTA, respectively. No phase separation was observed for DPPC:NTA-DODA [**Fig. 1(D)**]. However, a plateau region was revealed at high surface pressure, indicating that EDTA was squeezed out from the membrane.

Effect of EDTA on structural domain of lipid monolayer

To explore the EDTA effect on phase separation and domain formation of the lipid monolayer, Bodipy-PC was included in the film balance study. Domain structure and lateral organization of lipid mixtures were visualized by epifluorescence microscopy. As mentioned, the formation of DPPC domains was initiated at a surface pressure of 5 mN/m. Typical kidney-shaped and S-shaped solid domains were revealed upon further compression (**Fig. 2**). The addition of EDTA induced a slight change to the DPPC solid domains, so that the S-shaped domains appeared to transition into circular domains. An increase in size of the domain was observed upon further compression. However, a strong correlation between fluidization and expansion effects of EDTA on the lipid isotherm [**Fig. 1(A)**] and lateral organization of lipid molecules was revealed. The

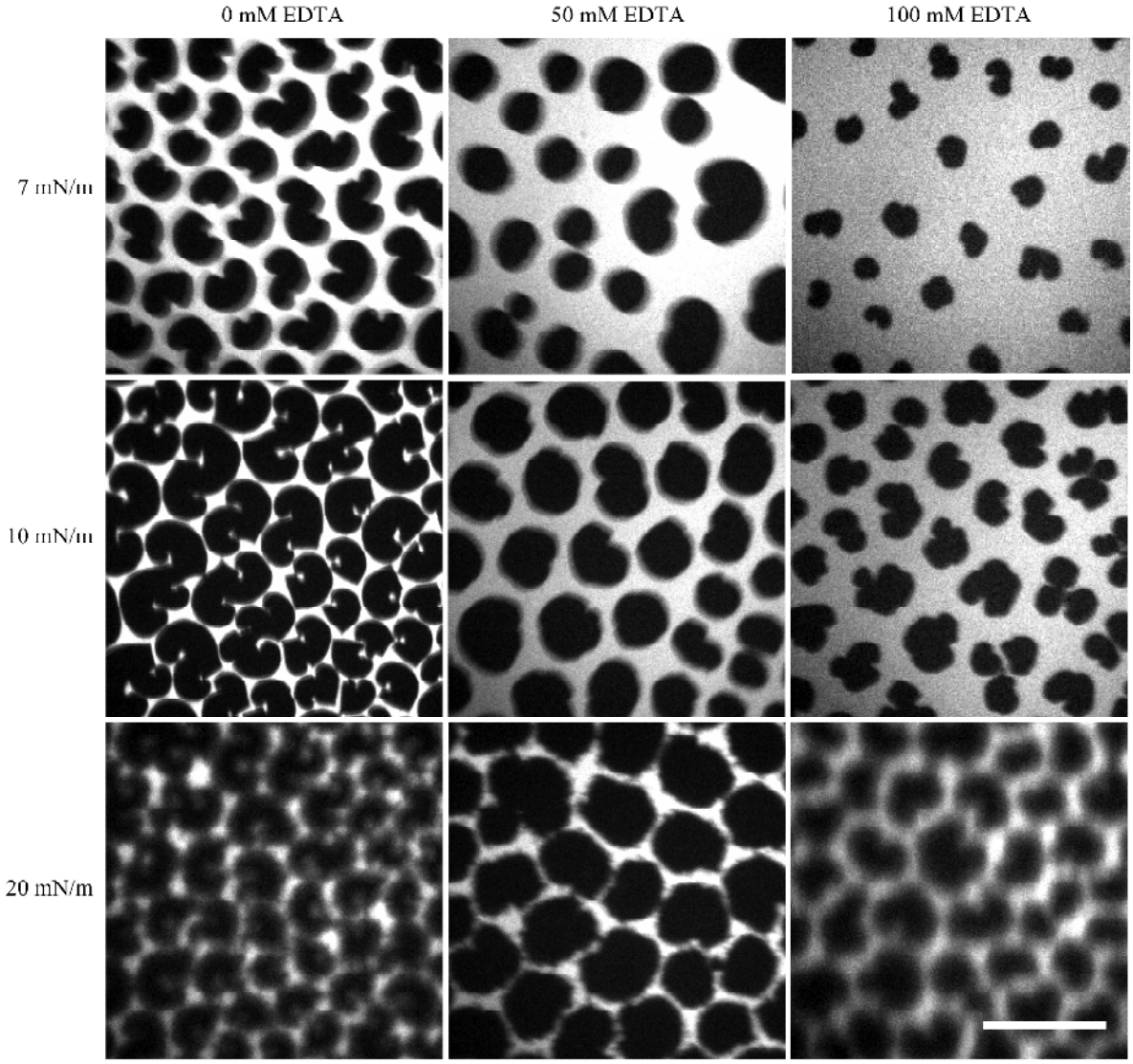

Fig. 2 Epifluorescence measurements of the 1,2-dipalmitoyl-*sn*-glycero-3-phosphocholine monolayer

These measurements were carried out in the absence and presence of 50 and 100 mM EDTA compressed at 7, 10, and 20 mN/m. Subphase was 10 mM HEPES and 150 mM NaCl, pH 7.5 with and without 50 and 100 mM EDTA. The scale bar (lower right corner) is 50 μm.

presence of EDTA decreased the size of the rigid domain and expanded the surface area of the liquid phase in a concentration-dependent manner (**Fig. 2**).

The structural domain of the DPPC:NTA-DODA mixture showed a distinctive morphology difference from pure DPPC (**Fig. 3**). A disturbance at the corner of rigid dark domains was observed. This inferred the behavioral organization of NTA-DODA on the DPPC monolayer, where localization occurred at the rim of the DPPC rigid domain. Such localization can be attributed to the presence of a bulky NTA head group, which limits the incorporation of NTA-DODA into the internal part of the domains. Importantly, a typical domain structure of DPPC was retrieved in the presence of EDTA. This supported the effect of EDTA on segregation of DPPC molecules from lipid mixtures. Higher EDTA concentration exerted a more potent effect on fluidization and expansion of surface area as represented by formation of small rigid domains.

With respect to the epifluorescence micrographs of DPPC:NTA-DOGS, rigid domain structures started to appear at a surface pressure of 10 mN/m (**Fig. 4**). DPPC:NTA-DOGS is comprised of a larger area of the *le* phase than the pure DPPC or DPPC:NTA-DODA at the same compression pressure (**Figs. 2–4**). Such findings support

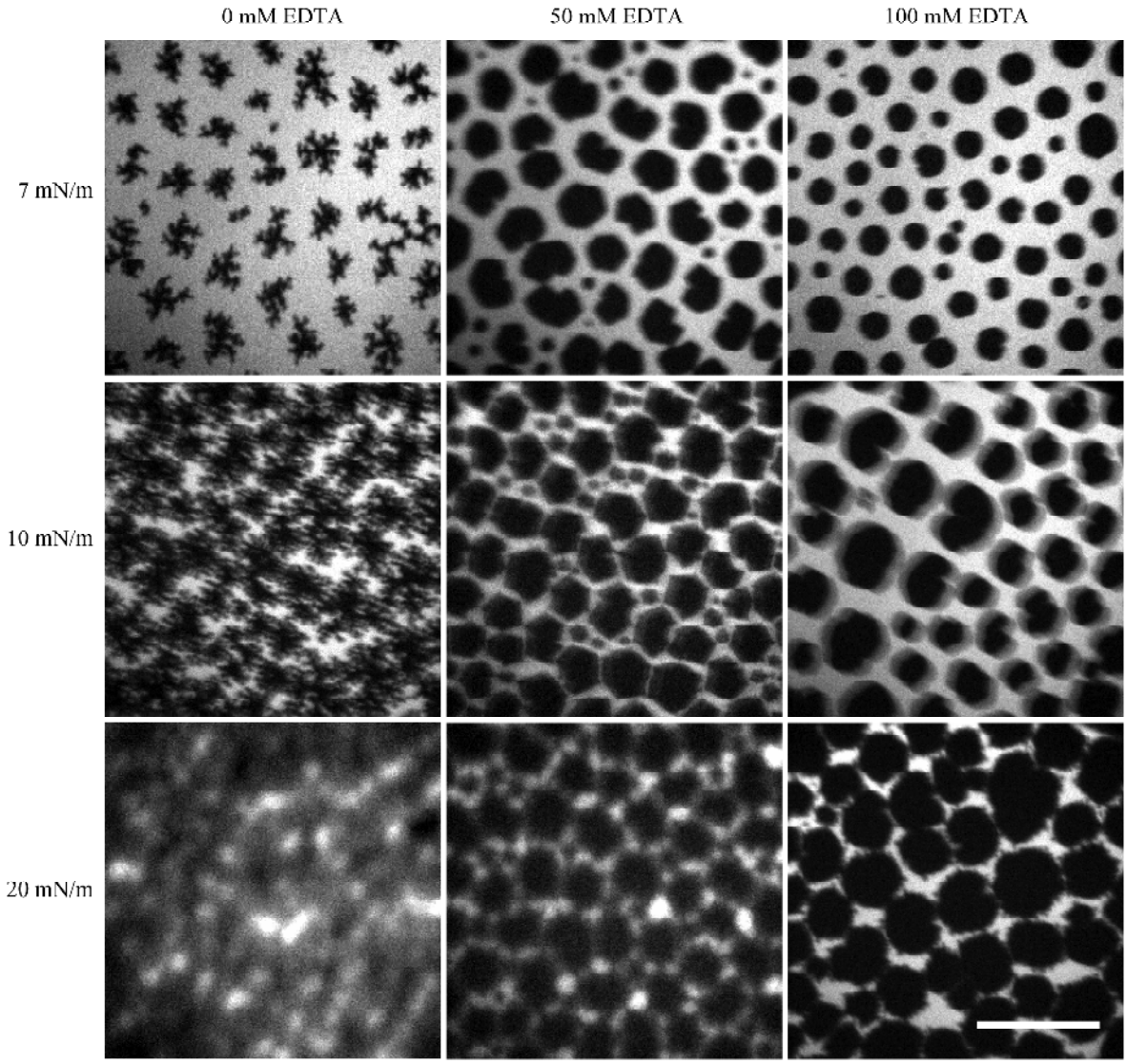

Fig. 3 Epifluorescence measurements of the 1,2-dipalmitoyl-*sn*-glycero-3-phosphocholine (DPPC):N^{α},N^{α}-Bis[carboxymethyl]-N^{ε}-[(dioctadecylamino)succinyl]-*L*-lysine (NTA-DODA) monolayer (4:1 molar ratio)

These measurements were carried out in the absence and presence of 50 and 100 mM EDTA compressed at 7, 10, and 20 mN/m. Subphase was 10 mM HEPES and 150 mM NaCl, pH 7.5 with and without 50 and 100 mM EDTA. The scale bar (lower right corner) is 50 μm.

the fluidization effect of the unsaturated hydrocarbon chain of NTA-DOGS in correspondence with the pressure-area isotherm [**Fig. 1(D)**]. The presence of EDTA in the subphase facilitated domain formation in a concentration-dependent fashion. EDTA was found to induce phase separation of the lipid mixture by decreasing the surface pressure required for *lc* formation. This is supported by the presence of low surface pressure at the plateau region [**Fig. 1(D)**]. Further compression of up to 20 mN/m revealed identical shape and size of the rigid domains supplemented with 50 and 100 mM EDTA, as well as high fluidity on the membranes [**Fig. 1(D)**].

It is uncertain whether a small amount of EDTA will exert any effect on the lipid membrane. To answer this question, a lipid film containing 4:1 molar ratio of DPPC: NTA-DOGS was used as a model. A pressure-area isotherm of lipid mixture spread on the PBS subphase revealed identical features similar to that of HEPES buffer (**Fig. 5**). However, a slightly more pronounced *le-lc* plateau region at 10 mN/m was observed (A_{20}=64 Å^2). A fluidization effect as well as expansion of the surface area of up to 69 Å^2 was found in the presence of 5 mM EDTA.

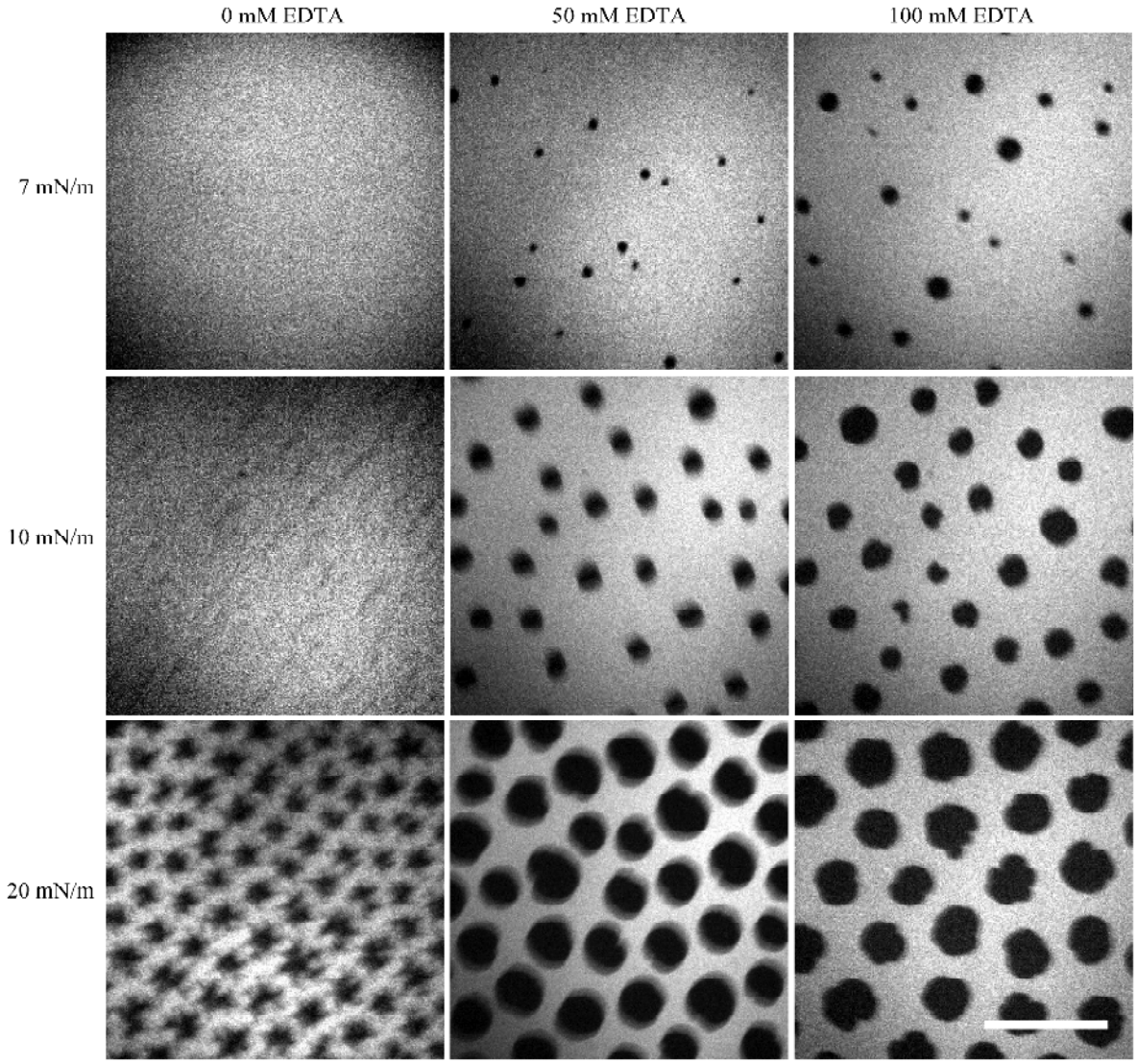

Fig. 4 Epifluorescence measurements of the 1,2-dipalmitoyl-*sn*-glycero-3-phosphocholine (DPPC):1,2-dioleoyl-*sn*-glycero-3-[*N*-(5-amino-1-carboxypentyl iminodiacetic acid) succinyl] (NTA-DOGS) monolayer (4:1 molar ratio)

These measurements were carried out in the absence and presence of 50 and 100 mM EDTA compressed at 7, 10, and 20 mN/m. Subphase was 10 mM HEPES and 150 mM NaCl, pH 7.5 with and without 50 and 100 mM EDTA. The scale bar (lower right corner) is 50 μm.

This evidence coincides with the 1 mM EGTA-supplemented monolayer as previously reported [29].

Influence of EDTA on surface topology of lipid membrane

To further investigate the detailed effect of EDTA on lipid membranes, AFM was used to visualize the surface topology of the lipid monolayer at the nanoscale level. As shown in **Fig. 6(A)**, a flat topology of solid-supported membrane was obtained indicating perfect film formation. Incubation of the membrane with 5 mM EDTA for 5 min gave rise to knob structures with a height and diameter of 3 and 150 nm, respectively. Continuous enlargement of the protrusion structure was found to be time-dependent. At 30 min, the knob structure was elongated, as represented by the length and width of approximately 400 and 200 nm, respectively. However, a slight increase in height was revealed (about 4 nm) during the 60 min observation. This infers an equilibrium state of interaction between EDTA and the lipid membrane. A possible explanation for the film protrusion could be the insertion of EDTA into the lipid layer, inducing membrane

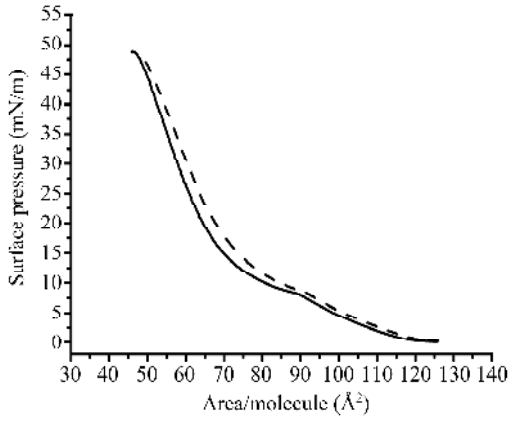

Fig. 5 The effect of EDTA on the lipid membrane

Pressure-area isotherms of the DPPC:NTA-DOGS monolayer in a molar ratio of 4:1 in the absence (solid line) and presence of 5 mM EDTA (dashed line). Subphase was 50 mM Na_2HPO_4 and 0.3 M NaCl, pH 7.4 with and without 5 mM EDTA.

curvature, as illustrated by the membrane protrusion on AFM images [**Fig. 6(B–D)**].

Kinetic monitoring of chelating activity of EDTA on lipid membrane

In addition to the lipid intercalation property, the chelating activity of EDTA was also investigated on a DPPC:NTA-DOGS membrane coated on the surface of a mass sensing device, namely a QCM. The sequestering effect of EDTA could then be monitored in real time. Zn^{2+} was added to the solid-supported membrane to mimic membrane-bound metal ions within biological systems. The metal-binding H_6GFP was then applied as a membrane-anchored protein by interacting with the membrane-bound Zn^{2+}. This resulted in a rapid decrease of resonance frequency up to 90 Hz [**Fig. 7(A)**]. Addition of 1 mM EDTA caused the resonance to recover to the baseline. However, a low level of non-specific adsorption of proteins on the lipid membrane was revealed. This indicated the association of H_6GFP to the membrane by Zn binding. The non-specific interaction was much lower than the interaction by the metal binding site [20]. The non-specific absorption of H_6GFP was confirmed upon injection of H_6GFP onto a zinc-free membrane, shown by a small reduction of resonance frequency of 20 Hz [**Fig. 7(B)**]. Prolonged exposure of EDTA (without zinc ions) resulted in the increase of the resonance frequency over the original level of up to 80 Hz, resulting in the loss of membrane materials from the resonator surface. This can be attributed to the direct interaction of EDTA with the biological membrane, as well as the sequestering effect.

Discussion

Although EDTA has been used as a food and drug additive in a variety of applications for decades, the molecular mechanism of interaction of EDTA with biological macromolecules, particularly to lipid membranes, has not yet been extensively studied. We report for the first time the interaction of EDTA with artificial lipid membranes using a combination of four biophysical approaches. Based on our findings, fluidization and protrusion of a lipid component, as provoked by the effects of EDTA in intercalating lipid membranes and sequestering metal ions, have been proven to play major roles in membrane disruption. This subsequently leads to membrane destabilization and cell lysis.

Film balance and epifluorescence investigations revealed strong fluidization and expansion of the lipid surface area in the presence of EDTA (**Figs. 1–5**). These findings agree with recent studies that EDTA and boric acid promote corneal penetration of the antiglaucoma drug through the transcellular pathway by increasing membrane fluidity [30, 31]. This can be explained by the molecular interaction of the lipid head group with EDTA molecules. Molecular modeling of the DPPC-EDTA complex suggests that EDTA tends to intercalate between phospholipid molecules through salt bridge formation, involving the positive ammonium group of choline and the carbonyl group of EDTA (**Fig. 8**). Salt bridges are a special form of strong hydrogen bonds, playing a crucial role in the structure and function of proteins [32]. The presence of a salt bridge is identified according to the proposed method by Kumar and Nussinov [33] as charged group atoms with opposite partial charges within a distance of 3.5 Å. The measured distances of hydrogen-bonded salt bridges between EDTA and DPPC are in the range of 1.32–2.06 Å (**Fig. 8**). Our molecular model of the DPPC-EDTA complex supports the notion that EDTA is capable of interacting with the polar head group of DPPC. The calculated 3-D model shows that the carboxylate oxygen of EDTA is engaged in electrostatic interactions with the choline amino hydrogen and the phosphate hydroxyl of DPPC. This indicates strong interaction between EDTA and the lipid head group, which correlates with the results from the pressure-area isotherm that some of the EDTA remains attached to the monolayer under a high surface pressure up to 45 mN/m [**Fig. 1(A,C,D)**]. Furthermore, insertion of EDTA into the lipid membrane expands the surface area and influences the structural domain organization (**Figs. 2–4**).

Due to the limitation of area available on a lipid

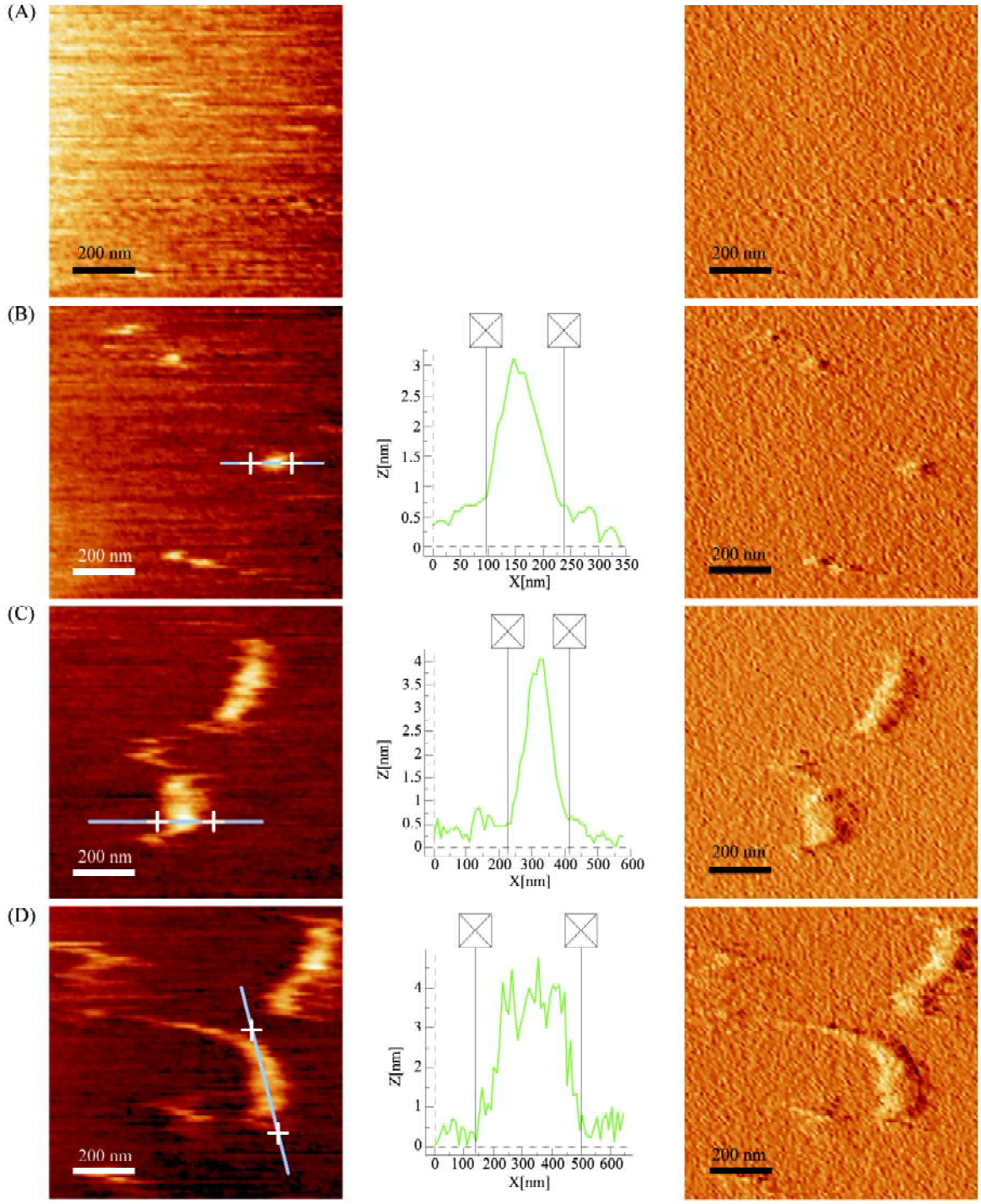

Fig. 6 The detailed effect of EDTA on lipid membranes by AFM

Topographical images (left), height analysis (center), and deflection images (right) of DPPC/DPPC:Zn^{2+}-NTA-DOGS (4:1) in the absence of EDTA (A) and in the presence of 5 mM EDTA incubated for 5 min (B), 30 min (C), and 60 min (D).

membrane, intercalation of EDTA into the lipid head groups introduces mechanical stress to lipid organization, inducing membrane curvature and protrusion (**Fig. 6**) [21]. The protrusion is then discharged from the lipid membrane, followed by membrane rearrangement [**Fig. 7(B)**]. The proposed mechanism of EDTA-induced membrane

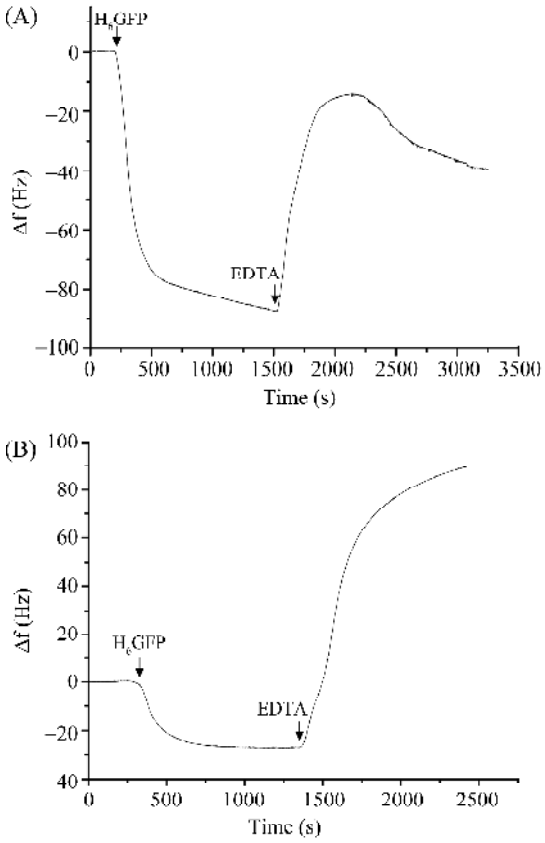

Fig. 7 Kinetic monitoring of chelating activity of EDTA on lipid membrane

Time-course of the resonance frequency change (ΔF) of 4:1 DPPC:NTA-DOGS coated quartz crystal microbalance chip after addition of phosphate-buffered saline containing 1 mM EDTA in the presence of specifically immobilized molecule (A) and non-specifically adsorbed molecule (B).

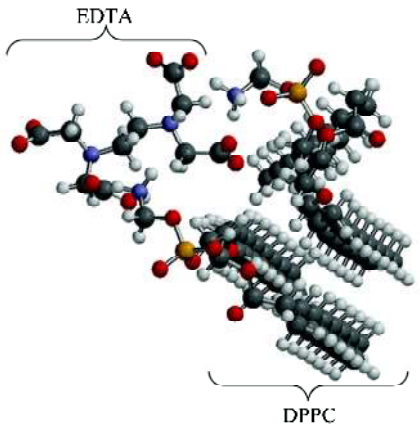

Fig. 8 Computer modeling representation of salt bridge formations between EDTA and 1,2-dipalmitoyl-*sn*-glycero-3-phosphocholine

Salt bridge formations are shown in this ball-and-stick diagram (top view orientation focusing on the intercalation part). Atoms of carbon, oxygen, phosphorus, nitrogen, and hydrogen are colored grey, red, orange, blue, and white, respectively.

fluidization and destabilization is schematically depicted in **Fig. 9**. Supportive evidence of the protrusion and detachment of membrane material has been reported. Release of lipopolysaccharide (LPS) molecules and membrane proteins from the outer membrane of *E. coli* in the presence of EDTA has also been observed [34]. Protein and phospholipid are released from the small intestine or colon membrane in rats after exposure to EDTA [35,36]. In other circumstances, the loss of breast milk cells, the

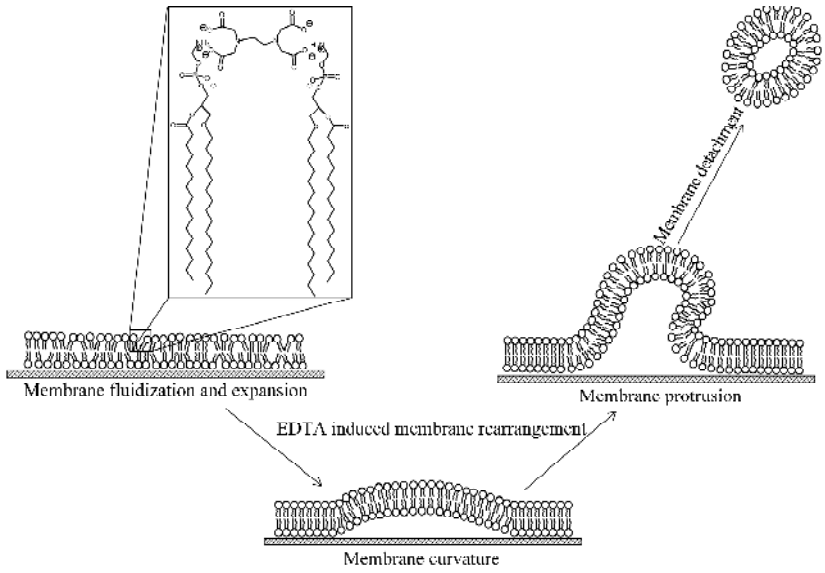

Fig. 9 Schematic representation of the plausible mechanism of EDTA-induced fluidization and permeabilization of lipid membrane

disruption of milk fat globules, and the release of membrane-bound proteins have already been investigated [37]. Our findings shed light on the molecular mechanism of membrane disruption, the leakage of cell constituents [37, 38], the induction of cell detachment [39], and the reduction of cell viability caused by EDTA [40]. Therefore, much attention should be focused on the use of EDTA in biological systems.

Using QCM, the destabilization effect of EDTA on lipid membranes can be monitored in real time. The chelating activity of EDTA on membrane-bound proteins has been revealed. The association of H_6GFP to the lipid membrane through Zn^{2+} is rapidly diminished after exposure to EDTA [**Fig. 7(A)**]. This indicates the disruption of protein and membrane association through the sequestering effect of EDTA. In many cases, membrane stabilization can be affected due to loss of protein association. The attachment of annexins and pentaxins to a lipid membrane through calcium ions has been proven to stabilize the membrane structure [41,42]. Actin filaments in cooperation with calcium ions establish a well-organized plasma membrane [43]. Moreover, membrane stabilization is also found in human serum albumin to protect erythrocytes from membrane damage due to mechanical tension [44]. Data from confocal fluorescence microscopy and electrical resistant measurements indicated that EDTA causes disruption of tight junction proteins of rat corneal membranes. This is revealed by the depletion of Ca^{2+} ions in the membrane followed by loosening of the tight junctions [13]. Bacterial outer membrane disintegration caused by EDTA has also been observed. It has been claimed that EDTA removes divalent cations from the LPS, resulting in the release of a significant proportion of LPS and causing membrane instability [45]. Moreover, a direct effect of EDTA on membrane stabilization has been validated in our experiments. EDTA induces a dramatic loss of material, as observed in the Zn^{2+}-free system [**Fig. 7(B)**]. This indicates a direct interaction of EDTA with the membrane (**Fig. 9**). In conclusion, both chelation and direct insertion effects of EDTA, in many cases, cause membrane destabilization.

References

1 Gyliene O, Aikaite J. Formation of binuclear EDTA and Cu(II) complexes in aqueous solutions. Polish J Chem 2003, 77: 99–104

2 Deucher GP. EDTA chelation therapy: An antioxidant strategy. J Advancement Med 1988, 1: 182–190

3 Chappell LT, Stahl JP. The correlation between EDTA chelation therapy and improvement in cardiovascular function: A meta-analysis. J Advancement Med 1993, 6: 139–160

4 Hancke C, Flytlie K. Benefits of EDTA chelation therapy on artherosclerosis: A retrospective study of 470 patients. J Advancement Med 1993, 6: 161–171

5 Whittaker P, Vanderveen JE, Dinovi MJ, Kuznesof PM, Dunkel VC. Toxicological profile, current use, and regulatory issues on EDTA compounds for assessing use of sodium iron EDTA for food fortification. Regul Toxicol Pharmacol 1993, 18: 419–427

6 Aamoth HL, Butt FJ. Maintaining food quality with chelating agents. Ann NY Acad Sci 1960, 88: 526–531

7 Bothwell TH, MacPhail AP. The potential role of NaFeEDTA as an iron fortificant. Int J Vitam Nutr Res 2004, 74: 421–434

8 Green S, Mazur A, Shorr E. Mechanism of the catalytic oxidation of adrenaline by ferritin. J Biol Chem 1956, 220: 237–255

9 Sakabe I, Paul S, Dansithong W, Shinozawa T. Induction of apoptosis in Neuro-2A cells by Zn^{2+} chelating. Cell Struct Funct 1998, 23: 95–99

10 Ivemark B, Seldinger SI. Renal damage in rats from the lead salt of EDTA and from umbradil. Acta Radiol 1957, 48: 366–375

11 Kane MH, Rodman JS, Horten B, Reckler J, Marion D, Vaughan ED Jr. Urothelial injury from ethylenediaminetetraacetic acid used as an irrigant in the urinary tract. J Urol 1989, 142: 1359–1360

12 Cranton EM. Kidney effects of ethylene diamine tretraacetic acid (EDTA): A literature review. J Advancement Med 1989, 2: 227–233

13 Rojanasakul Y, Liaw J, Robinson J. Mechanisms of action of some penetration enhancers in the cornea: Laser microscopic and electrophysiology studies. Int J Pharm 1990, 66: 131–142

14 Haque H, Russell AD. Effect of ethylenediaminetetraacetic acid and related chelating agents on whole cells of gram-negative bacteria. Antimicrob Agents Chemother 1974, 5: 447–452

15 Haque H, Russell AD. Effect of chelating agents on the susceptibility of some strains of Gram-negative bacteria to some antibacterial agents. Antimicrob Agents Chemother 1974, 6: 200–206

16 Helander IM, Alakomi HL, Latva-Kala K, Koski P. Polyethyleneimine is an effective permeabilizer of Gram-negative bacteria. Microbiology 1997, 143: 3193–3199

17 Alakomi HL, Saarela M, Helander IM. Effect of EDTA on *Salmonella enterica* serovar Typhimurium involves a component not assignable to lipopolysaccharide release. Microbiology 2003, 149: 2015–2021

18 Post A, Nahmen AV, Schmitt M, Ruths J, Riegler H, Sieber M, Galla HJ. Pulmonary surfactant protein C containing lipid films at the air-water interface as a model for the surface of lung alveoli. Mol Membr Biol 1995, 12: 93–99

19 Trommeshauser D, Galla HJ. Interaction of a basic amphipathic peptide from the carboxyterminal part of the HIV envelope protein gp41 with negatively charged lipid surfaces. Chem Phys Lipids 1998, 94: 81–96

20 Isarankura Na Ayudhya CI, Prachayasittikul V, Galla HJ. Binding of chimeric metal-binding green fluorescent protein to lipid monolayer. Eur Biophys J 2004, 33: 522–534

21 Prachayasittikul V, Isarankura Na Ayudhya C, Tantimongcolwat T, Galla HJ. Nanoscale orientation and lateral organization of chimeric metal-binding green fluorescent protein on lipid membrane determined by epifluorescence and atomic force microscopy. Biochem Biophys Res Commun 2005, 326: 298–306

22 Prachayasittikul V, Na Ayudhya CI, Hilterhaus L, Hinz A, Tantimongcolwat T, Galla HJ. Interaction analysis of chimeric metal-binding green fluorescent protein and artificial solid-supported lipid membrane by quartz crystal microbalance and atomic force microscopy. Biochem Biophys Res Commun 2005, 327: 174–182

23 Schmitt L, Dietrich C, Tempe R. Synthesis and characterization of chelator-lipids for reversible immobilization of engineered proteins at self-assembled lipid interfaces. J Am Chem Soc 1994, 116: 8485–8491

24 Dietrich C, Schmitt L, Tampe R. Molecular organization of histidine-tagged

biomolecules at self-assembled lipid interfaces using a novel class of chelator lipids. Proc Natl Acad Sci USA 1995, 92: 9014–9018

25 Dorn IT, Pawlitschko K, Pettinger SC, Tampe R. Orientation and two-dimensional organization of proteins at chelator lipid interfaces. Biol Chem 1998, 379: 1151–1159

26 Prachayasittikul V, Isarankura Na Ayudhya C, Mejare M, Bülow L. Construction of a chimeric histidine6-green fluorescent protein: Role of metal on fluorescent characteristics. Thammasat Int J Sci Tech 2000, 5: 61–68

27 Prachayasittikul V, Isarankura Na Ayudhya C, Bülow L. Lighting *E. coli* cells as biological sensors for Cd^{2+}. Biotechnol Lett 2001, 23: 1285–1291

28 de Silva S, de Silva RM, de Silva KMN. Molecular mechanics (MM), molecular dynamics (MD) and semi-empirical study of Co^{2+}, Cu^{2+}, Ni^{2+} and Cd^{2+} binding to N-terminal of human serum albumin (HSA). J Mol Struct 2004, 771: 73–81

29 Ross M, Steinem C, Galla HJ, Janshoff A. Visualization of chemical and physical properties of calcium-induced domains in DPPC/DPPS Langmuir-Blodgett layers. Langmuir 2001, 17: 2437–2345

30 Kikuchi T, Suzuki M, Kusai A, Iseki K, Sasaki H. Synergistic effect of EDTA and boric acid on corneal penetration of CS-088. Int J Pharm 2005, 290: 83–89

31 Kikuchi T, Suzuki M, Kusai A, Iseki K, Sasaki H, Nakashima K. Mechanism of permeability-enhancing effect of EDTA and boric acid on the corneal penetration of 4-[1-hydroxy-1-methylethyl]-2-propyl-1-[4-[2-[tetrazole-5-yl] phenyl]phenyl] methylimidazole-5-carboxylic acid monohydrate (CS-088). Int J Pharm 2005, 299: 107–114

32 Kumar S, Wolfson HJ, Nussinov R. Protein flexibility and electrostatic interactions. IBM J Res Dev 2001, 45: 499–512

33 Kumar S, Nussinov R. Salt bridge stability in monomeric proteins. J Mol Biol 1999, 293: 1241–1255

34 Amro N, Kotra L, Mesthrige K, Bulychev A, Mobashery S, Liu G. High-resolution atomic force microscopy studies of the *Escherichia coli* outer membrane: Structural basis for permeability. Langmuir 2000, 16: 2789–2796

35 Yamamoto A, Uchiyama T, Nishikawa R, Fujita T, Muranishi S. Effectiveness and toxicity screening of various absorption enhancers in the rat small intestine: Effects of absorption enhancers on the intestinal absorption of phenol red and the release of protein and phospholipids from the intestinal membrane. J Pharm Pharmacol 1996, 48: 1285–1289

36 Uchiyama T, Sugiyama T, Quan YS, Kotani A, Okada N, Fujita T, Muranishi S *et al*. Enhanced permeability of insulin across the rat intestinal membrane by various absorption enhancers: Their intestinal mucosal toxicity and absorption-enhancing mechanism of N-lauryl-β-*D*-maltopyranoside. J Pharm Pharmacol 1999, 51: 1241–1250

37 Ogundele MO. Cytotoxicity of EDTA used in biological samples: effect on some human breast-milk studies. J Appl Toxicol 1999, 19: 395–400

38 Elferink J. The effect of ethylenediaminetetraacetic acid on yeast cell membranes. Protoplasma 1974, 80: 261–268

39 Vogel KG. Effects of hyaluronidase, trypsin, and EDTA on surface composition and topography during detachment of cells in culture. Exp Cell Res 1978, 113: 345–357

40 Sceiza MF, Daniel RL, Santos EM, Jaeger MM. Cytotoxic effects of 10% citric acid and EDTA-T used as root canal irrigants: An *in vitro* analysis. J Endod 2001, 27: 741–743

41 Nelsestuen GL, Ostrowski BG. Membrane association with multiple calcium ions: Vitamin-K-dependent proteins, annexins and pentraxins. Curr Opin Struct Biol 1999, 9: 433–437

42 Bandorowicz-Pikula J. Lipid-binding proteins as stabilizers of membrane microdomains – possible physiological significance. Acta Biochim Pol 2000, 47: 553–564

43 Selden LA, Kinosian HJ, Newman J, Lincoln B, Hurwitz C, Gershman LC, Estes JE. Severing of F-actin by the amino-terminal half of gelsolin suggests internal cooperativity in gelsolin. Biophys J 1998, 75: 3092–3100

44 Zavodnik YB, Piletskaia TP, Stepuro II. Mechanical lysis of human erythrocytes. Membrane stabilization by plasma proteins. Ukr Biokhim Zh 1991, 63: 72–78

45 Leive L. Release of lipopolysaccharide by EDTA treatment of *E. coli*. Biochem Biophys Res Commun 1965, 21: 290–296

Edited by
Christopher YIP